ARCHIVES
of
FOUNDRY ENGINEERING
10.24425/afe.2025.155390
Published quarterly as the organ of the Foundry Commission of the Polish Academy of Sciences
ISSN (2299-2944)
Volume 2025
Issue 4/2025
133 – 143
18/4

Structure and Properties of Joints of an Yttrium-Containing Magnesium Alloy (WE43) Obtained by Friction Stir Welding

J. Adamiec, K. Łyczkowska *, K. Baluch, K. Gładyś, A. Mrowiec, G. Kopeć
Silesian University of Technology, Poland
* Corresponding author: E-mail: katarzyna.lyczkowska@polsl.pl

Received 04.09.24; accepted in revised form 06.05.25; available online 31.12.2025

Abstract

WE43 alloy belongs to a group of magnesium alloys with great potential for use in the automotive and aerospace industries. The industrial applicability of a material is determined, among other things, by its joinability. It was found that the treatment had a significant effect on the structure. The tensile strength of the FSW joints was at 75% of the base material's strength. All joints cracked in the weld. Both the base material and the weld exhibited high corrosion resistance in an atmosphere simulating automobile engine exhaust gases. The tests demonstrated that FSW technology can be used for joining and repairing WE43 gravity castings used in the automotive industry.

Keywords: Friction stir welding (FSW), Magnesium alloy, WE43, Joining technology, Heat treatment

1. Introduction

Magnesium alloys can be divided into wrought alloys and casting alloys (Figure 1). The most commonly chosen magnesium alloys are those with aluminum. One of the directions for improving the properties of magnesium alloys, and especially their creep resistance, is the addition of rare earth elements [1,2].

WE43 and WE53 are magnesium-based alloys with the addition of rare earth elements and yttrium (Mg-Y-RE-Zr). These alloys are characterized by high creep resistance, which allows them to operate at temperatures up to 250°C over long periods, while during short exposures, they can be used even at temperatures up to 300°C [3,4]. Magnesium alloys from the WE series can be used for components of racing car engines operating under high loads and temperatures, and even for high-reliability components of aircraft drive systems, which must be characterized by high strength and corrosion resistance [5-7].

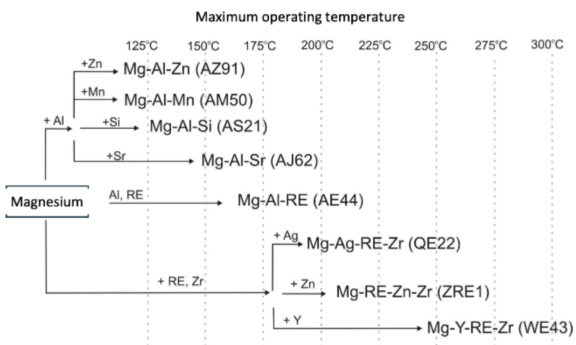

Fig. 1. Development of magnesium alloys [7]

Table 1.
Selected properties of WE43 alloy according to ASTM B80 and for heat no. 20091842 [8,9]

Chemical composition [%]													
Standard	Zn	Si	Cu	Mn	Fe	Ni	Li	Zr	Y	Nd	RE	Other	Mg
ASTM B80	-	-	-	-	-	-	-	min. 0.4	3.7-4.3	-	2.4-4.4	-	balance
Batch 20091842	0.01	0.01	0.004	<0.01	0.002	0.004	0.01	0.51	3.7	2.2	0.96	<0.01	balance
Mechanical properties													
Standard		R_m [MPa]			$R_{e0.2}$[MPa]				A_5 [%]			HV3	
ASTM B80		min. 250			min. 172				min. 2			80-107	
Batch 20091842		250			178				7			85	

The primary alloying additions in WE43 (designation according to ASTM B80) are yttrium and a mixture of rare earth elements, mainly neodymium. The chemical composition of WE43 alloy and its mechanical properties are shown in Table 1 [8,9].

Yttrium is added to enhance the alloy's mechanical properties at ambient and elevated temperatures and to increase creep resistance [8,10-12], whereas rare earth elements raise the allowable operating temperature. In alloy WE43, the mixture of rare earth elements consists of 85% neodymium and about 15% praseodymium. These elements increase strength at elevated temperatures through the precipitation of stable strengthening phases both within and at the boundaries of α-Mg grains [13,14]. Additionally, neodymium improves the fluidity of magnesium alloys, reduces shrinkage porosity, and slightly increases tensile strength [15].

The microstructure of WE43 alloy in the as-cast condition consists of α-Mg solid solution grains, eutectic Mg(α)+β ($Mg_{12}NdY$) and phase precipitates with varying contents of the alloying additions: the irregularly shaped $Mg_{41}Nd_5$ phase, rectangular precipitates of the MgY phase, elongated precipitates of the $Mg_{24}Y_5$ phase, and precipitates of the intermetallic β phase ($Mg_{12}NdY$) (Figure 2a) [16].
The heat treatment of WE43 alloy is aimed at enhancing its mechanical properties and en-compasses solution heat treatment and aging. The manufacturer recommends solution heat treatment at 525°C for 8 hours, followed by cooling in air or hot water [11]. The aging should be conducted at 250°C for 16 hours and be followed by cooling in air. As a result of the solution treatment, the intermetallic phase precipitates dissolve in the alloy's matrix and the solid solution grains increase in size (Figure 2b).

Among the basic technologies for joining components made of magnesium alloys, including large castings, are Tungsten Inert Gas (TIG) welding and Metal Inert Gas (MIG) welding. Friction Stir Welding (FSW) is also used.

The classic and most frequently performed joining of the WE43 alloy using TIG welding technology has been described in numerous works [17-21]. Authors Wang Q, Tong X, and others, in their research, fabricated the EV33 alloy using O-TIG and PC-TIG welding, respectively. The effects of welding current and pulse current frequency on the welded joints were systematically evaluated in the aspects of microstructural evolution and mechanical properties [17]. In another research [18], the effects of TIG welding process on the microstructure, the tensile properties and the fatigue strength of ZE41(Mg–Zn–RE–Zr) magnesium alloy were investigated. In case of the TIG welded samples, a grain refinement in the fusion zone and a grain coarsening in the heat affected zone takes place. The distributions of the micro-hardness reflect the microstructure variations occurred in the welded samples. Comparing data on TIG welding of magnesium alloys, it can be asserted that magnesium alloys with the addition of rare earth elements can be considered weldable. However, the main difficulty encountered is hot cracking of these materials [19].

a)
b)
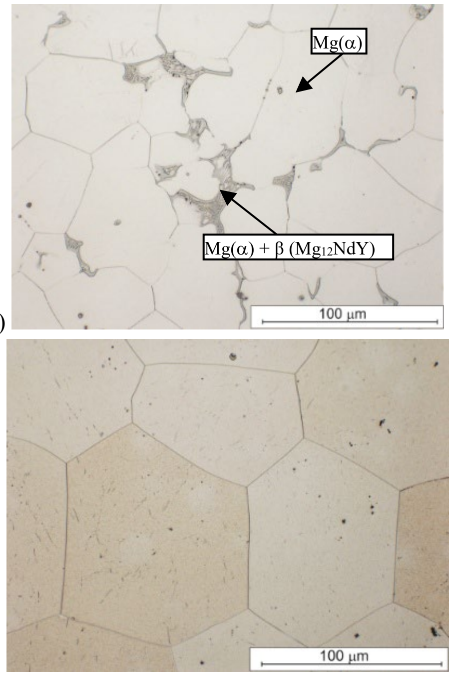

Fig. 2. Microstructure of WE43 alloy: a) in as-cast condition, b) following solution heat treatment and aging in air at 250ºC for 16 h [17]

The Friction Stir Welding (FSW) technology, used for joining lightweight metal alloys, including aluminum and magnesium alloys, ensures the production of joints free from hot cracking, as the process occurs within the material's plasticizing temperature range and not above the solidus temperature [20-22]. In a few studies [19,23,24], the influence of MIG and TIG welding technologies on the WE43 alloy has been described. In the study [19], the author indicated that the main issue in joining is hot cracking, and welding should be conducted on the material in a supersaturated state. Meanwhile, the authors in [23] provided an overview of the welding possibilities for magnesium alloys, primarily from the Mg-Al group. They concluded that fusion and solid-state welding processes of these alloys are discussed with emphasis on mechanical characterization. Laser welding is the most effective fusion welding technique for most Mg alloys whereas, the predominant solid-state method is friction stir welding. The importance of process variables such as heat inputs, welding velocity (speed) and post weld treatments on the microstructural evolution, on mechanical and physical properties of the distinct zones of the weld joints are described. The weldment is the most susceptible to failure due to phase transformation, defects such as microporosity and relatively coarse grain sizes after solidification. In the work [24] it was found that optimizing welding parameters such as current, time, force, tool profile, travel speed, etc., is crucial for enhancing the overall performance of aluminum/magnesium dissimilar alloy welding and has demonstrated successful welding outcomes. Furthermore, refining the welding process itself can also lead to a substantial enhancement in the quality of welds.

In solid phase aluminum/magnesium welding using an intermediate layer, it has been found that metals with a high melting point can effectively resist contact between liquid aluminum and magnesium, thereby hindering the formation of aluminum magnesium intermetallic compounds. Moreover, by using an intermediate layer metal that undergoes an aluminum–magnesium metallurgical reaction, alloying can be achieved, leading to a change in the composition of the compound phase in the welded joint, making it a promising area for further development [24].

FSW is primarily used for joining large-sized castings in the automotive and aerospace industries. Such joints are created through the heating, plasticizing, and deformation of components by a rotating tool that moves along the joint line (Figure 3) [25]. The joining of the material occurs in the solid state, below the melting temperature [26-27]. The heat required to form the weld is generated by the friction of the tool's working surfaces (the pin and the shoulder) against the surfaces of the joined pieces, as well as by the internal friction of the deformed metals. Mutual friction welding of both materials occurs in the welding area, creating a joint with a characteristic structure.

An FSW joint consists of a heat-affected zone, where precipitation processes can occur, a thermomechanically affected zone, and a heavily deformed weld area with a clearly visible weld nugget (Figure 4) [28,29].

The advantages of FSW technology include low joining temperature, absence of shrinkage, absence of hot cracking, minor structural deformation following the welding process, good mechanical properties, and the capability to join work pieces ranging from 1.5 mm to 60 mm in thick-ness [25]. The drawbacks of the FSW process include the need for rigid fixation of the work pieces, low welding speeds, and the possibility of incomplete mixing of the materials on the root side [30,31].

The FSW process is described in the literature and is recommended for magnesium alloys. However, these studies mainly focus on alloys from the magnesium-aluminum group [32,33]. Few works on joining the WE43 alloy using FSW technology are limited to the selection of welding parameters and a basic description of structural changes [34,35]. Comprehensive and detailed studies on the welding of WE43 alloy castings are lacking. The joining of castings, both high-pressure castings for the automotive industry and large-scale castings, is one of the key areas of development for FSW technology for magnesium alloys. Data analysis indicates substantial potential for the implementation of this technology in the aerospace and automotive industries for joining castings with rolled elements. However, there is a necessity for a thorough description of the changes in the structure of the FSW joint, as well as an evaluation not only of its mechanical properties but also of its service properties, such as resistance to high-temperature corrosion, specifically around 200–300 °C, which simulates engine exhaust gas environments. Since a two-step heat treatment (solution treatment and aging) is prescribed for magnesium alloys, it is also important to describe the joining possibilities at each stage of the heat treatment, which affects the ability to achieve a joint meeting the requirements of designers.

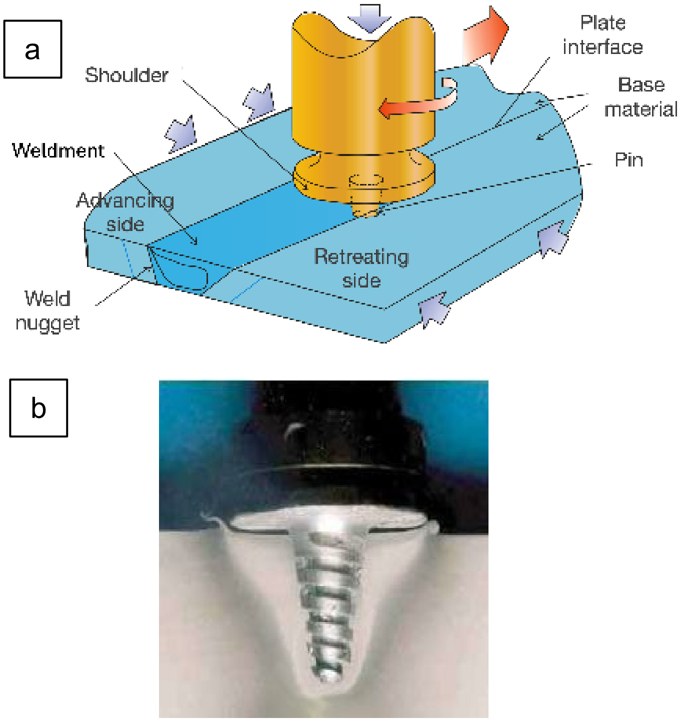

Fig. 3. FSW process: a) diagram of the FSW method, b) Whorl™ tool [25,27]

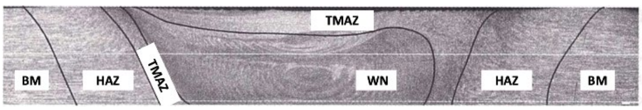

Fig. 4. Structure of an FSW weld: a) weld zones, where: WN – weld nugget, TMAZ – thermomechanically affected zone, HAZ – heat-affected zone, BM – base material [28]

This paper presents the results of tests on the properties of FSW joints of WE43 alloy and examination of structural changes occurring in such joints following two variants of heat treatment. The study is a significant supplement to the information available in the literature and provides guidelines for designing FSW joints of WE43 alloy.

2. Materials and Methods

The specimens used for the tests were joints of plates made from WE43 alloy coming from heat no. 20091842 produced by Magnesium Elektron. A comparison of the chemical composition of heat no. 20091842 with the requirements of the ASTM B80 standard confirmed that the material tested met the specifications for WE43 alloy (Table 1).

The 5 mm thick test plates were cut from a gravity casting and FSW-welded, without prior heat treatment, at the Łukasiewicz Research Network of the Upper Silesian Institute of Technology [36] (Figure 5). The work [36] provides a detailed description of the tool and welding technology used. A commercial conical tool known as Triflute™ was employed to create the joint. This tool is characterized by a conical shape of the mixing pin, featuring three cutouts that facilitate material mixing during the welding process. The design of this tool allows for the movement of less material during welding, enabling an increase in welding speed while maintaining high joint quality. Additionally, the cutouts in the pin effectively "tear" the material in the weld zone, which leads to an increase in heat generation. The joints were then used for metallographic examinations aimed at assessing their initial structure and changes in that structure following two heat treatment variants: solution heat treatment (Variant 1) and solution heat treatment followed by aging (Variant 2) (Table 2).

Table 2.
Heat treatment parameters applied for the tested FSW joints of WE43 alloy.

Heat treatment variant	Heat treatment parameters
Base material	No heat treatment
Variant 1	Solution treatment at 525°C for 8 hours followed by cooling in air
Variant 2	Solution treatment at 525°C for 8 hours followed by cooling in air; aging at 250°C for 16 hours followed by cooling in air

It was assumed that following various heat treatment variants, the properties of FSW (Friction Stir Welding) joints, including plasticity and strength, would undergo changes. As a reference variant, a joint without any heat treatment was adopted, for which it was assumed that the strength should be at the level of 0.7 of the base material strength, i.e., the WE43 alloy in the as-cast condition. This value was established based on data pertaining to aluminum alloys welded using the FSW method, as well as research results for aluminum alloy joints welded using arc welding methods [37,38]. Solution treatment of the WE43 alloy FSW joint leads to the dissolution of intermetallic phases (Variant 1), which, as a result of this process, alters the properties of the entire joint. Conversely, the aging process causes the precipitation of intermetallic phases with the assumed volume fraction, size, and distribution (Variant 2). The homogenization and strengthening of the joint structure through full heat treatment are expected to enhance the mechanical properties of the joint. However, such data are not available in the literature. Therefore, acquiring this information constitutes a significant contribution to the field of materials engineering and joining technologies, which is particularly important for process engineers and designers in the context of designing or repairing large-scale castings and the appropriate selection of heat treatment.

Examples of the test joints are shown in Figure 5. Following the metallographic examinations, specimens for static tensile tests were cut from the joints. The mechanical tests were complemented by fractographic examinations and hardness measurements.

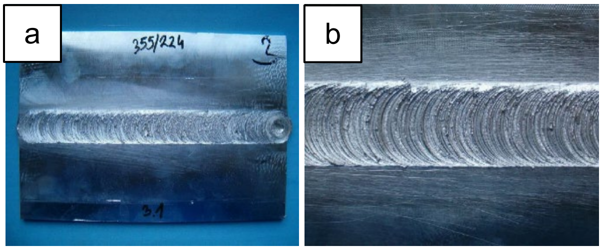

Fig. 5. FSW joint made of WE43 casting alloy: a) view of the weld face, b) weld face with visible friction welding lines

A major factor determining whether FSW joints of WE43 alloy can be used in industrial applications is the alloy’s resistance to high-temperature corrosion in gas environments such as exhaust gases. As part of the study, corrosion resistance tests were conducted in an atmosphere simulating exhaust gases at 300°C. The results obtained led to conclusions that enable the design and construction of WE43 components for the automotive and aerospace industries.

3. Structure of FSW joints of WE43 alloy

Structural changes determine the operational properties of a joint and thus the feasibility of using FSW welding technology to join WE43 castings or repair casting defects. The specimens used for the structural analysis were cut perpendicular to the welding direction and then ground and polished according to the procedure described in paper [1]. The metallographic examinations were conducted using a light microscope in bright field mode, at magnifications of up to 500x. Examples of the observed macro- and microstructures are shown in Figure 6.

Treatment	Base material	Advancing zone	Weld nugget	HAZ
No heat treatment	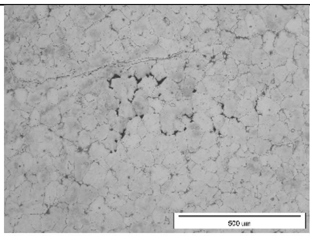	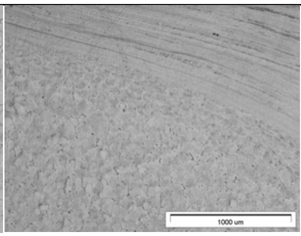	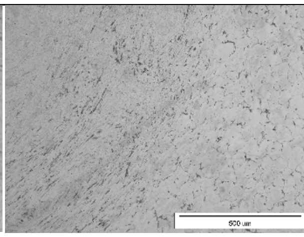	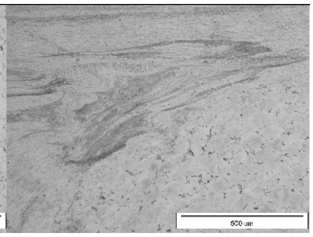
Solution treatment: 8h/525°C air	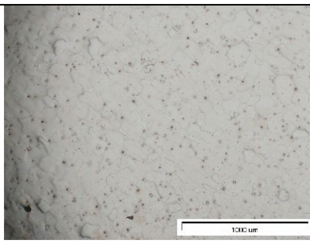	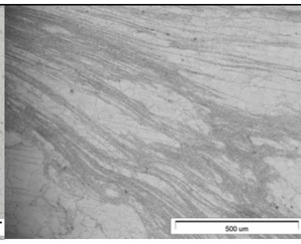	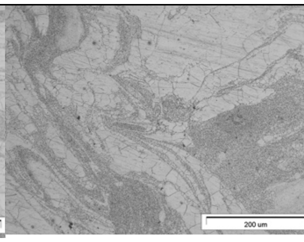	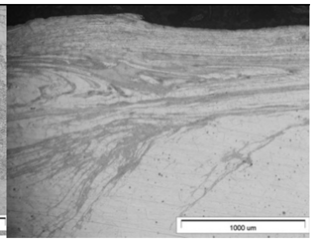
Solution treatment: 8h/525°C air Aging: 16h/250°C air	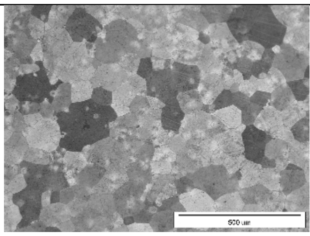	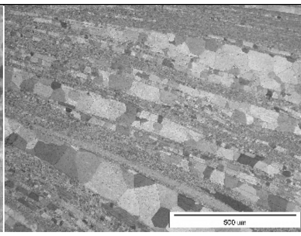	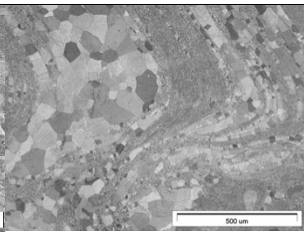	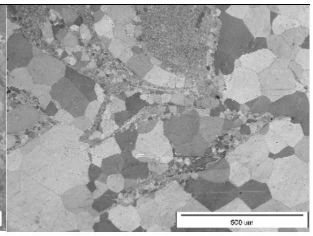

Fig. 6. Microstructure of FSW joints of WE43 alloy depending on the heat treatment variant

Microanalysis of the chemical composition of the phases revealed in the FSW joints was per-formed using energy-dispersive X-ray spectroscopy (EDS) at 15kV on a Hitachi Thermo Noran System Six analyzer used in conjunction with a HITACHI S-4200 scanning electron microscope. Examples of the results are shown in Figure 7. The phase analysis was conducted using X-ray dif-fraction on a JEOL JDX-7S diffractometer equipped with a copper anode lamp (λCuKα = 1.54178 Å, 20 mA, 40 kV) and a graphite monochromator. The data was recorded in the 2θ range between 10° and 90°, with 0.05° steps, at 5s/step. The phases were identified based on information from the International Centre for Diffraction Data (ICDD) database (Figure 8).

During the microstructural examinations, a eutectic mixture [Mg(α) + β ($Mg_{12}NdY$) + Mg_5RE] was revealed at the boundaries of the solid solution of RE elements in the Mg(α) phase (Figures 7a, 8a). Solution treating the alloy at 525°C causes this eutectic mixture to dissolve. Following the solution treatment, the structure showed sparse precipitates of MgY and $Mg_{12}Y$ phases. Following aging at 250°C for 16 hours, a single-phase Mg(α) solid solution structure with fine β phase ($Mg_{12}NdY$) precipitates was observed (Figs. 7b, 8b).

During the FSW welding process, a significant grain refinement occurred in the stir zone, followed by the dissolution of the fragmented Mg(α) + β (Mg12NdY) eutectic mixture during the solution treatment. Following the solution treatment and aging, areas of grain recrystallization were revealed in the welding areas where plastic deformation had occurred (Figure 6).

4. The effect of heat treatment on the properties of FSW joints of WE43 alloy

The FSW joints were subjected to heat treatment in two variants. In Variant 1, the joints were solution treated at 525°C for 8 hours and then air-cooled. In Variant 2, after solution treating, the joints were additionally aged at 250°C for 16 hours and then air-cooled (Table 2). From those joints, specimens for static tensile tests were prepared (Figure 9). The static tensile tests were performed on a Zwick Z600E strength testing machine in accordance with the requirements of the PN-EN ISO 6892-1 standard. Examples of results are shown in Figure 10 and summarized in Table 3.

a)

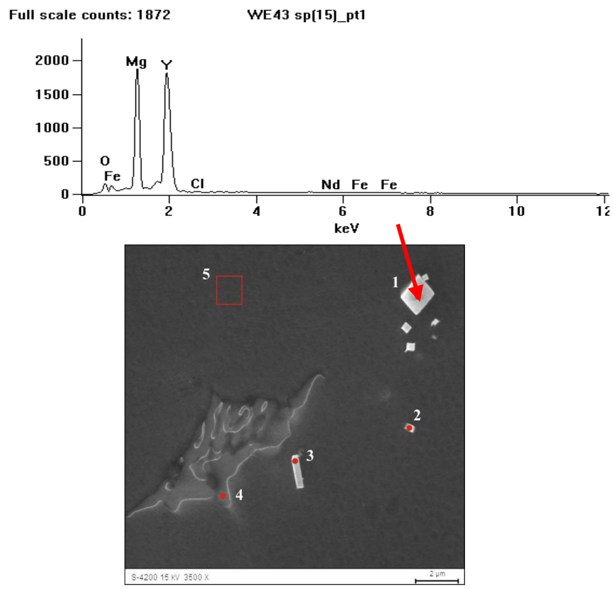

Chemical composition	Element		
wt.%	Mg	Y	Nd
Point 1	27.61	69.12	2.80
Point 2	60.52	32.94	6.55
Point 3	70.26	23.34	5.41
Point 4	77.18	8.99	13.84
Point 5	95.50	4.50	0.00

b)

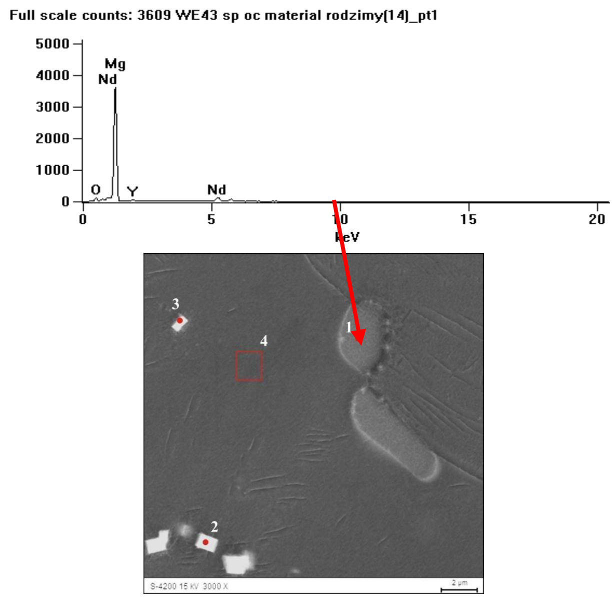

Chemical composition	Element		
wt.%	Mg	Y	Nd
Point 1	74.23	2.75	23.02
Point 2	42.94	52.41	4.65
Point 3	55.19	44.82	0.00
Point 4	95.84	4.16	0.00

Fig. 7. Results of the microanalysis of the chemical composition of the precipitates revealed in FSW joints of WE43 alloy: a) no heat treatment (initial condition), b) following solution heat treatment and aging (parameters provided in Table 2)

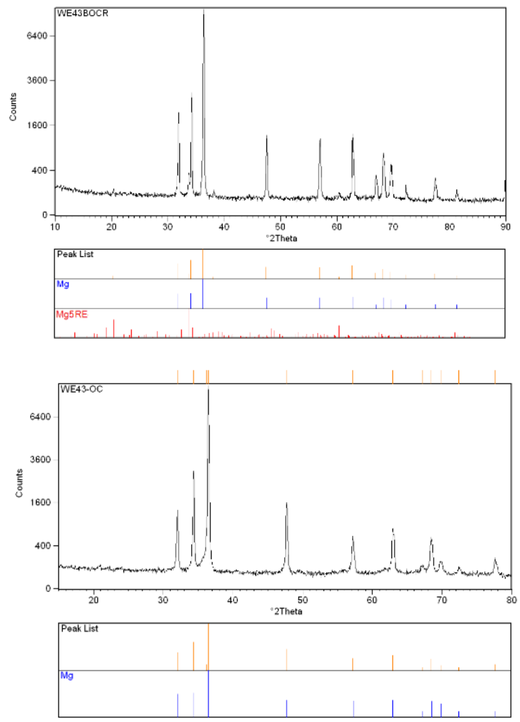

Fig. 8. XRD diffractograms of an FSW joint of WE43 alloy: a) base material, no heat treatment, b) material following solution heat treatment and aging (parameters provided in Table 2).

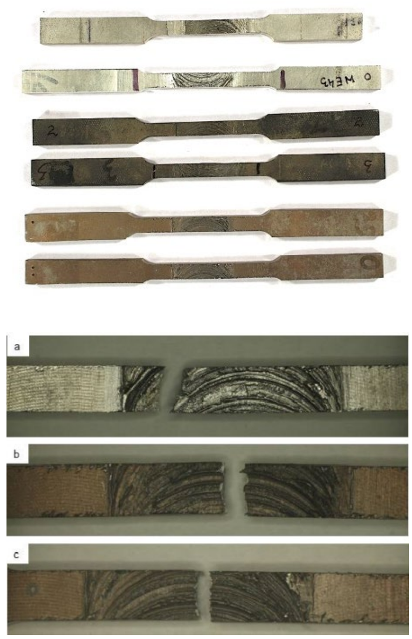

Fig. 9. Examples of static tensile test specimens cut from FSW joints of WE43 alloy following the different heat treatment variants and views of the fracture sites: a) no heat treatment, b) solution heat treatment, c) solution heat treatment and aging (parameters provided in Table 2)

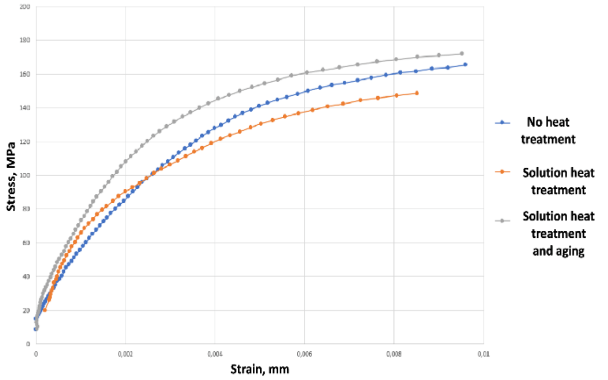

a)

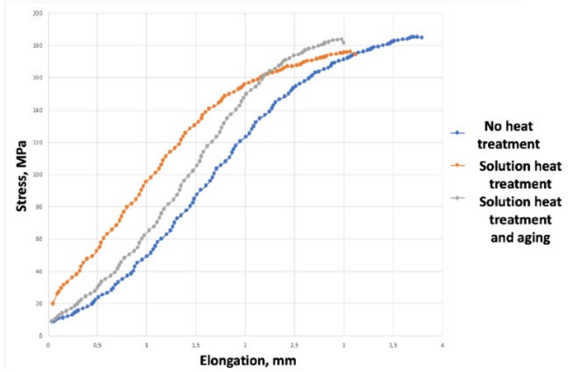

b)

Fig. 10. Examples of tensile curves for FSW joints of WE43 alloy following the different heat treatment variants: a) strain as a function of stress, b) elongation as a function of stress

Table 3.
Results of the static tensile tests of FSW joints of WE43 alloy

Heat treat-ment: Variant	Width b [mm]	Thickn-ess a [mm]	Cross-section area S_0 [mm2]	Length L_0 [mm]	Yield point $R_{p0,2}$ [MPa]	Tensile strength R_m [MPa]	Elon-gation A_5 [%]
No HT	5.84	5.98	34.9	40	143	185	9
1	6.05	6.27	37.9	40	112	176	3
2	6.25	6.25	39.1	40	143	184	2

The static tensile strength tests were complemented by examinations of the fracture surfaces performed using a Joel 6000 scanning electron microscope (SEM) in secondary electron (SE) mode, which allows for the observation of fracture topography. Figure 11 shows fracture surfaces for the non-heat-treated specimens and the specimens subjected to full heat treatment, i.e., solution treatment and aging. Based on the tests conducted, it was found that the strength (R_m) of the non-heat-treated joints was 185 MPa, the yield strength (R_e) was 142 MPa, and the elongation (A_5) was at 9%. Following solution treating, the strength properties of the joints decreased to R_m = 176 MPa, Re = 114 MPa, and elongation A_5 = 3%. Following solution treating and aging (full heat treatment), the strength increased to Rm = 184 MPa, the yield strength was R_e = 143 MPa, and the elongation was 2% (Table 3).

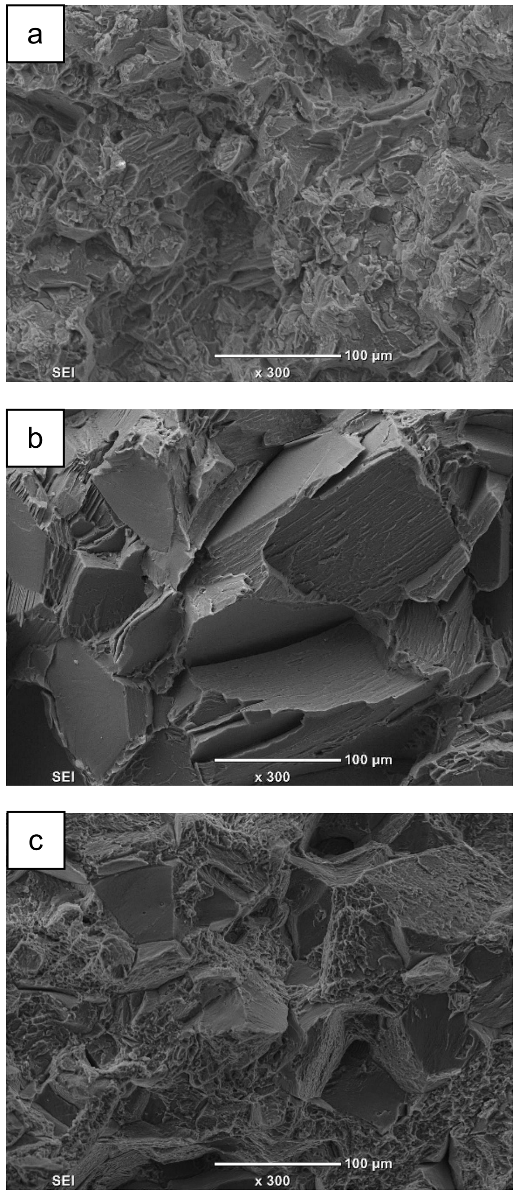

Fig. 11. Fracture surfaces following the static tensile strength tests: a) mixed fracture in the non-heat-treated specimen, b) brittle fracture in the solution treated specimen, c) mixed fracture in the solution treated and aged specimen.

The post-test analysis of the specimens revealed that all the joints fractured in the weld zone, which is characteristic of welded joints of magnesium alloys and aluminum alloys. The tensile strength of FSW joints of WE43 alloy is approximately 75% of the strength of the base material.

Fractographic examinations of the fracture surface of the non-heat-treated specimen revealed a fine-grained mixed fracture with clearly visible areas of transgranular fracture (Figure 11a). The fracture surface of the solution treated specimen showed typical brittle fracture characteristics, which is common for the coarse-grained single-phase structure that forms after the dis-solution of intermetallic phases (Figure 11b). In the case of the solution treated and aged specimen, the fracture was brittle, with a mixed transgranular and intergranular structure and clearly visible fine-grained areas, which was confirmed during the metallographic examinations of the joint structure (Figures 6, 11c).

5. High-temperature corrosion resistance of FSW joints of WE43 alloy

The high-temperature corrosion resistance tests were conducted in a gas mixture simulating the exhaust gas of a diesel car engine (chemical composition of the gas mixture: 9% O2 + 0.02% SO2 + 7% CO2 + 0.15% NO2 in nitrogen), at a temperature of 300°C. The test stand consisted of tube furnaces with quartz and ceramic tubes, reducers, gas sampling points with rotameters, a neutralizing system, and cylinders with the gases making up the simulated mixture (Figures 12a, b). The specimens cut from the joints were 5x5x3 mm in size. The measure of high-temperature corrosion resistance of FSW joints was defined as the change in the specimen mass following the test. The experiment was conducted over 1000 hours, with corrosion product mass gain measurements taken after 50, 100, 250, 500, 750, and 1000 hours. For each specimen, three mass measurements were taken and averaged. The standard deviation from the average was below 1%. The results of the mass change measurements are shown in Figure 13a.

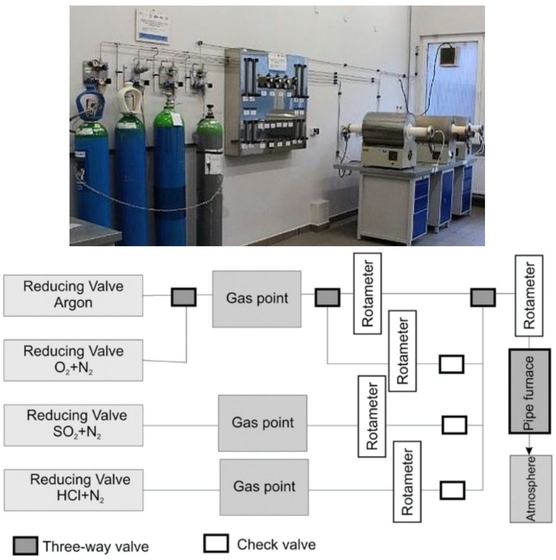

Fig. 12. Test stand for assessing high-temperature corrosion resistance at the Department of Metallurgy and Recycling, Silesian University of Technology: a) general view, b) diagram

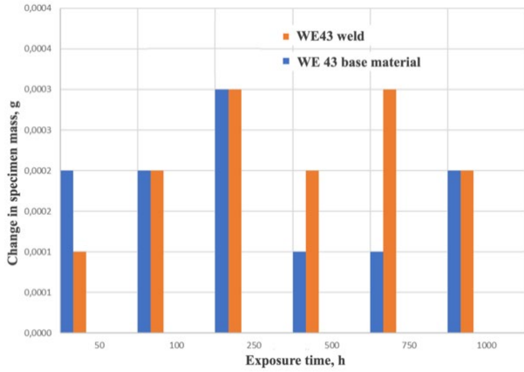

Fig. 13. Change in specimen mass as a function of time of exposure to a simulated exhaust gas atmosphere

Irrespective of the sampling site (base material or weld area) and the exposure time, the mass of the specimens remained virtually unchanged after 50, 100, 250, 500, 750, and 1000 hours (Figure 13). The minor differences in the specimens' mass (approx. 0 ÷ 0.03%) can be considered negligible and are attributable to measurement error, which was set at 0.1%. It was found that both WE43 alloy and FSW joints made from this alloy are resistant to the action of exhaust gases at temperatures of up to 300°C. This indicates that FSW technology can be successfully used to join WE43 components in the automotive industry.

6. Summary and conclusions

In Mg-Y-RE-Zr (WE) alloys, the primary alloying additions are yttrium, rare earth elements (RE), and zirconium. In WE43 alloy, the main component of the RE mixture is neodymium. The microstructure of Mg-Y-RE-Zr casting alloys consists of grains of a solid solution of yttrium (~0.7% at.) and neodymium (~0.3% at.) in magnesium and Nd-rich precipitates at grain boundaries. Zirconium particles are found within the Mg(α) grains. The as-cast structure of Mg-Y-RE-Zr alloys does not provide sufficient mechanical properties; therefore, heat treatment consisting of solutionizing and aging is applied to alloys of the Mg-Y-RE-Zr group [39]. Solutionizing of Mg-Y-Nd-Zr alloys is carried out at temperatures above 525°C, typically after an 8-hour preheating time [19, 40]. It was assumed that the properties of the Friction Stir Welding joint, including plasticity and strength, would change following various heat treatment variants. As a reference variant, a joint without any heat treatment was adopted, for which it was assumed that the strength should be at the level of 0.7 of the base material strength, i.e., the WE43 alloy in the as-cast condition. This value was established based on data pertaining to aluminum alloys welded using the FSW method, as well as research results for aluminum alloy joints welded using arc welding methods [37,38]. Solution treatment of the WE43 alloy FSW joint leads to the dissolution of intermetallic phases (Variant 1), which, as a result of this process, alters the properties of the entire joint. Conversely, the aging process causes the precipitation of intermetallic phases with the assumed volume fraction, size, and distribution (Variant 2). The homogenization and strengthening of the joint structure through full heat treatment are expected to enhance the mechanical properties of the joint. However, such data are not available in the literature. Therefore, acquiring this information constitutes a significant contribution to the field of materials engineering and joining technologies, which is particularly important for process engineers and designers in the context of designing or repairing large-scale castings and the appropriate selection of heat treatment.

One of the newest technologies for joining or repairing WE43 castings is Friction Stir Welding (FSW). The process involves stirring the base material in the solid state, which results in its joining. Based on study [38] and the results of the tests described in this paper, it was determined that the best properties of FSW joints of WE43 plates were achieved with a welding speed of 280 mm/min and the tool's rotational speed of 355 rpm, without heat treatment. These FSW welding parameters were used to produce WE43 alloy casting joints and to evaluate the effect of heat treatment on their properties.

The structure of the base material of the non-heat-treated FSW joint of WE43 alloy consisted of α-Mg solid solution grains, an α-Mg + β(Mg_5RE) eutectic mixture, and precipitates rich in yttrium and neodymium (Figure 7,8). In the weld area, a significant refinement of α-Mg solid solution grains and yttrium- and neodymium-rich precipitates was observed, with the surface fraction of the latter being less than 3% (Figure 6). Following solution heat treatment and aging (T6), partial recrystallization of the material occurred in the weld due to severe deformation. During aging, Mg_3Nd and $Mg_{12}Nd$ strengthening phases precipitated in the joint (Figure 6,7). For the non-heat-treated joints and the joints subjected to Variant 2, the strength was at 75% of the base material's strength, i.e., approximately 185 MPa (Table 3, Figure 10). A significant reduction in elongation A5 to 2% was observed, which was attributed to partial recrystallization of the joint area, resulting in grain growth (Figure 6). However, after solution treatment, the joint strength decreased to approximately 176 MPa, and elongation A5 reduced to 3% (Table 3). In all joints, irrespective of the heat treatment variant, the fracture occurred in the weld area (Figure 9). Fractographic analysis results confirm the metallographic observations. The results of fractographic investigations confirm the metallographic observations. The fracture surface clearly exhibits brittle fracture with coarser grains in the case of joints subjected to the first heat treatment variant, while a mixed fracture with a predominance of brittle characteristics is observed in the second heat treatment variant (Figure 11). Such structural changes in the FSW joint after T6 heat treatment indicate the necessity of limiting the operating temperature of the joined or welded large-scale castings to approximately 200 °C, due to the potential for significant grain growth resulting from the recrystallization process (Figures 6, 11). The grain growth in the mixing zone of the material in the FSW joint leads to increased brittleness of the joint, which is also supported by the results of the fractographic analysis (Figures 11b, c).

The results of mechanical properties testing for FSW joints without heat treatment, as well as aging (Variant I) and aging combined with solution treatment (Variant II) (Table 3), in comparison to similar joints produced by TIG welding as presented in reference [19], indicate that the properties of the WE43 alloy FSW joints are superior to those of joints welded with the TIG method. The mechanical properties of FSW joints are around 0.75 of the base material properties, while TIG-welded joints exhibit properties in the range of 0.50 to 0.55 of the base material properties. Both FSW joints and those produced using the TIG welding method do not require heat treatment.

Similar results were obtained for all joint zones and for the base material in the high-temperature corrosion resistance tests in a simulated exhaust gas atmosphere (9% O_2 + 0.02% SO_2 + 7% CO_2 + 0.15% NO_2 in nitrogen) at a temperature of 300°C, (the chemical composition and temperature of the gas are typical for the exhaust gases of a diesel engine), irrespective of the heat treatment variant.

A detailed analysis of mass changes in the samples following high-temperature corrosion resistance testing indicates similar resistance of the joints, irrespective of the heat treatment condition. The minor differences in joint mass observed after the tests are attributed to a loss of approximately 0.0002 g, which is negligible and results from the mechanical detachment of small corrosion products, primarily in the weld face area of the FSW joint.

The fact that the mass changes were very similar for all specimens demonstrates a good resistance of WE43 alloy and its FSW joints to high-temperature corrosion, confirming the feasibility of using this technology in the automotive industry. It is important to highlight that the results obtained from the corrosion resistance assessment in a simulated exhaust gas atmosphere are comparable to those of WE43 alloy joints welded using the TIG method [41, 42].

Based on the results of the tests conducted and the analysis of the literature, the following conclusions were formulated:

- In the WE43 alloy, the main alloying elements used are yttrium (3.7%) and neodymium (2.2%). Microstructural investigations of the WE43 alloy revealed the presence of a eutectic structure at the boundaries of the solid solution of rare earth elements in magnesium, specifically Mg(α) + β (Mg12NdY). Solution treatment of the alloy at 525°C leads to the dissolution of this eutectic. In the structure of the samples after post-solution treatment, a limited number of phase precipitates of MgY and Mg12Y were observed. After aging at a temperature of 250°C for 16 hours, a single-phase structure of the solid solution Mg(α) with fine precipitates of the β phase ($Mg_{12}NdY$) is observed.
- Heat treatment significantly affects the structure of an FSW joint of WE43 alloy. The base material without heat treatment has a structure comprising solid solution Mg(α) with inter-metallic phase precipitates and a eutectic mixture between the grains. During solution treatment, the intermetallic phases dissolve, and during aging, they precipitate. The size of the precipitates depends on the duration and temperature of the aging process.
- The strength of an FSW joint is about 75% of that of the base material, and ductility is below 10%. The best results were achieved for joints that were subjected to no heat treatment. Properly shaped joints were obtained with a welding speed of 280 mm/min and the tool's rotational speed of 355 rpm. On this basis, it can be concluded that FSW joints do not require post-welding heat treatment.
- Irrespective of the heat treatment applied, both the base material and the FSW joints are resistant to high-temperature corrosion (up to 300°C) in a simulated automotive engine exhaust atmosphere (9% O_2 + 0.02% SO_2 + 7% CO_2 + 0.15% NO_2 in nitrogen).

- FSW technology can be used in the automotive industry for joining or repairing WE43 castings.

Acknowledgements

The study was carried out as part of project SKN/SP/535438/2022, titled: "Innovative Technology for Joining an Yttrium-Containing Magnesium Alloy (WE43) by Friction Stir Welding". The project was co-funded by the Minister of Education and Science from the state budget under the program "Student Science Clubs Create Innovations and project no. 11/020/BK_24/0129 and 11/040/ BK_24/ 0036.

References

[1] Czerwiński, F. (2008). *Magnesium Injection Molding.* New York: Springer.

[2] Martynenko, N.S., Luk'Yanova, E.A., Morozov, M.M., Yusupov, V.S., Dobatkin, S.V. & Estrin, Y.Z. (2018). Study of the structure, mechanical properties and corrosion resistance of magnesium alloy WE43 after rotary swaging. *Metal Science and Heat Treatment*. 60(3), 253-258. DOI 10.1007/s11041-018-0269-3.

[3] Mengucci, P., Barucca, G., Riontino, G., Lussana, D., Massazza, M., Ferragut, R. & Aly, E. H. (2008). Structure evolution of a WE43 Mg alloy submitted to different thermal treatment. *Materials Science and Engineering*: A. 479(1-2), 37-44. https://doi.org/10.1016/j.msea.2007.06.016.

[4] Kang, H., Huang, Z.H., Wang, S.C., Yan, H., Chen, R.S. & Huang, J.C. (2020). Effect of pre-deformation on microstructure and mechanical properties of WE43 magnesium alloy II: Aging at 250 and 300 °C. *Journal of Magnesium and Alloys*. 8(1), 103-110. DOI.org/10.1016/j.jma.2019.11.012.

[5] Nie, J.F. & Muddle B.C. (2000). Characterization of strengthening precipitate phases in a Mg-Y-Nd alloy. *Acta Materialia*. 48(8), 1691-1703. DOI 10.1016/S1359-6454(00)00013-6.

[6] Beladi, H. & Bernett, M.R. (2007). Influence of aging pre-treatment on the compressive deformation of WE54 alloy. *Materials Science and Engineering* A. 452-453, 306-312. DOI /10.1016/j.msea.2006.10.125.

[7] Friedrich, H. & Schumann, S. (2001). Research for a "new age of magnesium" in the automotive industry. *Journal of Materials Processing Technology*. 117(3), 276-281. DOI 10.1016/S0924-0136(01)00780-4

[8] Friedrich, H.E., Mordike, B.L. (2006). *Magnesium Technology: Metallurgy, Design, Data, Applications*. Berlin - Heidelberg: Springer.

[9] Matweb. (2023). Retrieved December 11, 2023, from http://www.matweb.com/search/DataSheet.aspx?MatGUID=4b8a8c13cf354fc5893a40cf8eca022c&ckck=1.

[10] Mraied, H., Wangb, W. & Cai, W. (2019). Influence of chemical heterogeneity and microstructure on the corrosion resistance of biodegradable WE43 magnesium alloys. *Journal of Materials Chemistry* B. 7(41), 6399-6411. DOI.org/10.1039/C9TB00388F.

[11] Elektron WE-43. (2005-2006). Magnesium Elektron: Service & Innovation in Magnesium, 467.

[12] Pekguleryuz, M. O., & Kaya, A. A. (2003). Creep resistant magnesium alloys for powertrain applications. *Advanced Engineering Materials*. 5(12), 866–878.

[13] Yang, Z., Li, J.P., Zhang, J.X., Lorimer, G.W. & Robson, J. (2008). Review on research and development of magnesium alloys. *Acta Metallurgica Sinica (English Letters).* 21(5), 313-328. DOI: 10.1016/S1006-7191(08)60054-X.

[14] Yu, K., Li, W. & Wang, R. (2005). Mechanical properties and microstructure of as-cast and extruded Mg-(Ce, Nd)-Zn-Zr alloys. *Journal Central South University Technology*. 12(5), 499-502. DOI: 10.1007/s11771-005-0110-1.

[15] Avedesian, M., Baker, H. (1999). *Magnesium and Magnesium Alloys*. ASM Speciality Handbook.

[16] Kiełbus, A. (2007). The influence of solution treatment time on the microstructure of WE43 magnesium alloy. *Acta Metallurgica Slovaca*. 13, 653-657.

[17] Antion C., Donnadieu P., Perrard F., Deschamps, A., Tassin, C. & Pisch, A. (2003). Hardening precipitation in Mg-4Y-3RE alloy. *Acta Materialia*. 51(18), 5335-5348. DOI: 10.1016/S1359-6454(03)00391-4.

[18] Santos, T., Vilaça, P. & Quintino, L. (2008). Developments in ndt for detecting imperfections in friction stir welds in aluminium alloys. *Welding in the World*. 52(9), 30-37. https://doi.org/10.1007/BF03266666.

[19] Thomas, W.M., Nicholas, E.D., Needham, J.C., Murch, M.G., Temple-Smith P., Dawes, C.J. (1991). GB Patent Application nr 9125978.8. Friction Stir Butt Welding. Int. Patent Application no. PCT/GB92/02203.

[20] Zadroga, L., Pietras, A., Papkala, H. (2003). *Study and research on the conditions of joining dissimilar materials by modern friction welding methods.* Report on the research work no Bb-96. Welding Institute. Gliwice.

[21] Wang Q, Tong X., Wu G., Zhan J. Qi F., Zhang L., Liu W. (2023). Microstructure and strengthening mechanism of TIG welded joints of a Mg-Nd-Gd alloy: Effects of heat input and pulse current. *Materials Science and Engineering: A*. 869, 144816, 1-18. DOI.org/10.1016/j.msea.2023.144816.

[22] Peter, I., Rosso, M. (2018). Investigations on Tungsten Inert Gas Welded Magnesium Alloy In 7th International Conference on Advanced Materials and Structures – AMS, 28–31 March 2018. Romania, DOI 10.1088/1757-899X/416/1/012030.

[23] Adamiec J. (2010). *Weldability od magnesium alloy*, Monography. Gliwice, Poland: Silesian University of Technology.

[24] Palanivel S., Nelaturu P., Glass B. & Mishra R.S. (2015). Friction stir additive manufacturing for high structural performance through microstructural control in an Mg based WE43 alloy. *Materials & Design (1980-2015).* 65, 934-952. DOI.org/10.1016/j.matdes.2014.09.082.

[25] Li, J., Zhang, DT., Chai, F. & Zhang, W. (2020). Microstructures and mechanical properties of WE43 magnesium alloy prepared by friction stir processing. *Rare Metals*. 39, 1267-1272 https://doi.org/10.1007/s12598-014-0306-3.

[26] Wu, B., Yusof, F., Li, F., Abdul Razak, B. B., Bin Muhamad, M. R., Badruddin, I. A., Hussien, M., Kamangar, S. & Ibrahim, M. Z. (2024). Influence of friction stir processing parameters on microstructure, hardness and corrosion resistance of biocompatible Mg alloy WE43. *Arabian Journal for Science and Engineering.* 49, 1897-1911. DOI.org/10.1007/s13369-023-08037-8.

[27] Klenam, D. E. P., Ogunwande, G. S., Omotosho, T., Ozah, B., Maledi, N. B., Hango, S. I., Fabuyide, A.A., Mohlala, L., van der Marwe, J.W. & Bodunrin, M.O. (2021). Welding of magnesium and its alloys: an overview of methods andprocess parameters and their effects on mechanical behaviour and structural integrity of the welds. *Manufacturing Review*. 8, 29, 1-32. DOI.org/10.1051/mfreview/2021028.

[28] Chen, H., Zhu, Z., Zhu, Y., Sun, L., & Guo, Y. (2023). Solid-state welding of aluminum to magnesium alloys. *A review. Metals.* 13(8), 1410, 1-23. DOI.org/10.3390/ met13081410.

[29] Adamiec J., Zadroga L. & Chabko T. (2008). Sucture and properties of the AZ91 magnesium alloy welds created with the use of Friction Stir Welding (FSW). *Inżynieria Materiałowa*. 29(4), 320-325.

[30] Luty G. & Gałaczyński T. (2018). Joining technologies for aerospace structures, Part 2, Linear Friction Stir Welding (FSW). *Projektowanie i Konstrukcje Inżynierskie*. 11(134). (in Polish).

[31] Threadgill, P.L., Leonard, A.J., Shercliff, H.R. & Withers, P.J. (2009). Friction stir welding of aluminum alloys. *International Materials Reviews*. 54(2), 49-93. https://doi.org/10.1179/174328009X411136.

[32] Salih, O.S., Neate, N., Ou, H. & Sun, W. (2020). Influence of process parameters on the microstructural evolution and mechanical characterisations of friction stir welded Al-Mg-Si alloy. *Journal of Materials Processing Technology*. 275, 116366, 1-14. https://doi.org/10.1016/j.jmatprotec.2019.116366.

[33] Radisavljevic, I., Zivkovic, Z., Radovic, N. & Grabulov, V. (2013). Influence of FSW parameters on formation quality and mechanical properties of Al 2024-T351 butt welded joints. *Transactions of Nonferrous Metals Society of China*. 23(12), 3525-3539. https://doi.org/10.1016/S1003-6326(13)62897-6.

[34] Retrieved March 18, 2025, from http://www.twi.co.uk/technical-knowledge/published-papers/friction-stir-welding-of-magnesium-alloys-march-2003/

[35] Yang, Q., Xiao, B.L. & Ma, Z.Y. (2012). Influence of process parameters on microstructure and mechanical properties of friction-stir-processed Mg-Gd-Y-Zr Casting. *Metallurgical and Materials Transactions* A. 43(6), 2094-2109. https://doi.org/10.1007/s11661-011-1076-2.

[36] Feng, A.H. & Ma, Z.Y. (2009). Microstructural evolution of cast Mg–Al–Zn during friction stir processing and subsequent aging. *Acta Materialia*. 57(14), 4248-4260. https://doi.org/10.1016/j.actamat.2009.05.022.

[37] Badkoobeh, F., Mostaan, H., Rafiei, M., Bakhsheshi-Rad, H.R. & Berto, F. (2021). Friction stirwelding/processing of Mg-based alloys: a critical review on advancements and challenges. *Materials*. 14(21), 6726, 1-35. https://doi.org/10.3390/ma14216726.

[38] Singh, K., Singh, G. & Singh H. (2018). Review on friction stir welding of magnesium alloys. *Journal of Magnesium and Alloys*. 6(4), 399-416. https://doi.org/10.1016/j.jma.2018.06.001.

[39] Khan, Y.S., Abidi, M.H., Malik, W., Lone, N.F., Aboudaif, M.K. & Mohammed, M.K. (2023). Effect of traverse speed variation on microstructural properties and corrosion behavior of friction stir welded WE43 Mg alloy joints. *Materials.* 16(14), 4902, 1-14. DOI.org/10.3390/ma16144902.

[40] Węglowska, A., Matusiak, J., Miara, D., Pietrzak, J. (2022). *Research on the Friction Stir Welding process of cast magnesium alloys intended for operation at elevated temperatures.* Research report no. BW-52/22 (Bb136). Łukasiewicz Research Network – Upper Silesian Institute of Technology, Gliwice, Poland.

[41] Thakur, N. & Harvinder, L. (2015). Experimental comparison of tig and friction stir welding processes for aluminium 6063-T6. *International Journal on Emerging Technologies*. 6(2), 189-194.

[42] Singh, G., Kang, A.S., Singh, K. & Singh, J. (2017). Experimental comparison of friction stir welding process and TIG welding process for 6082-T6 aluminium alloy. *Materials Today Proceedings*. 4(2), 3590-3600. https://doi.org/10.1016/j.matpr.2017.02.251.